

Room-temperature Ferromagnetism, Half-metallicity and Spin Transport in Monolayer CrSc₂Te₄-Based Magnetic Tunnel Junction Devices

Ruixue Yue,^{†ab} Xuemin Su,^{†c} Xiaodong Lv,^{*ab} Bingwen Zhang,^d Shaolong Su,^{ab}

Haipeng Li,^{ab} Shaoqiang Guo^{*c} and Jian Gong^{*abe}

^a College of Physics and Electronic Information, Inner Mongolia Normal University, Hohhot, 010022, China

^b Inner Mongolia Key Laboratory for Physics and Chemistry of Functional Materials, Inner Mongolia Normal University, Hohhot, 010022, China

^c School of Physical Science and Technology, Inner Mongolia University, Hohhot 010021, China

^d Fujian Key Laboratory of Functional Marine Sensing Materials, Minjiang University, Fuzhou, 350108, China

^e Ordos Institute of Technology, Ordos, 017000, China

*Corresponding authors: 20230008@imnu.edu.cn (XL); shaoqiangguo@imu.edu.cn (SG); ndgong@imu.edu.cn (JG)

[†] R. Yue and X. Su contributed equally in this work.

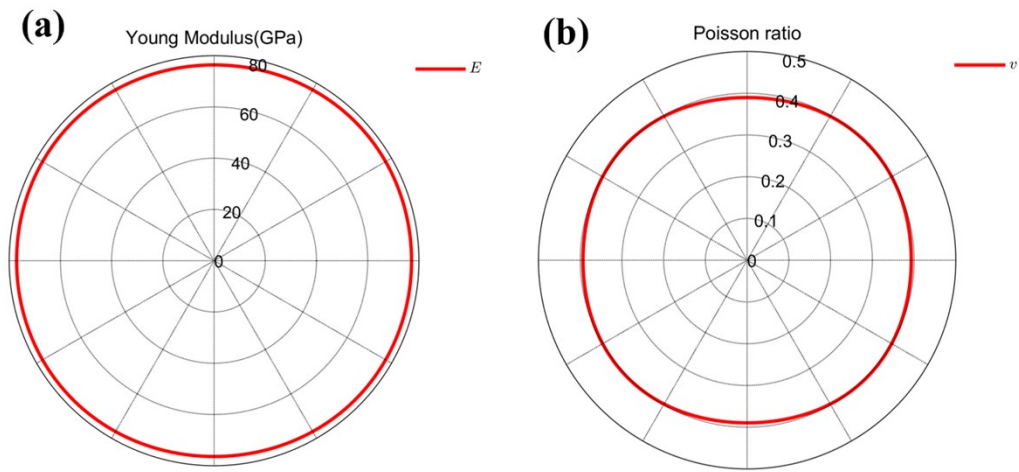


Fig. S1 Calculated orientation-dependent Young's modulus $Y(\theta)$ and Poisson's ratio $\nu(\theta)$ for CrSc_2Te_4 monolayer, respectively.

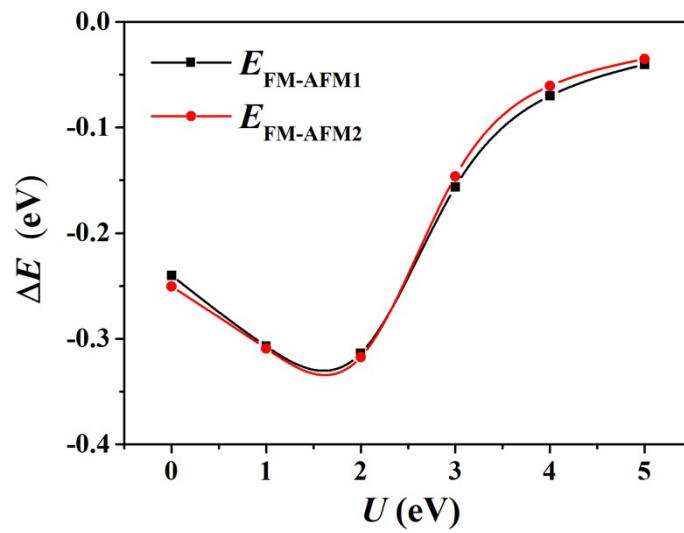


Fig. S2 The calculated energy differences between FM and AFM states for CrSc_2Te_4 monolayer with different U values using the PBE method.

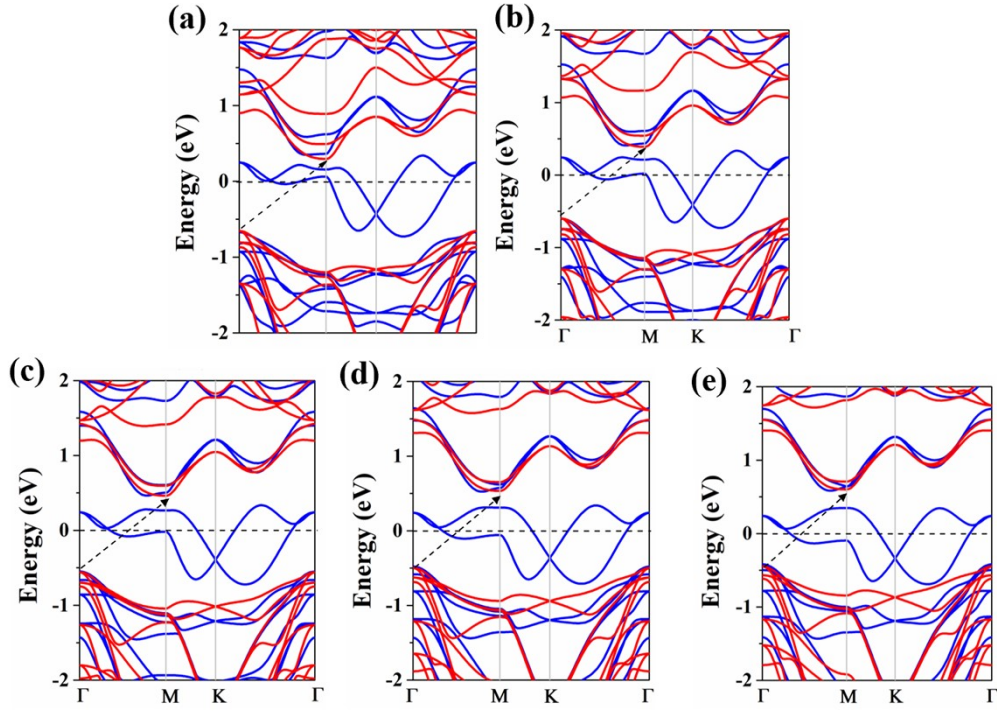


Fig. S3 The calculated band structures of CrSc_2Te_4 monolayer with different U values using the PBE method. The blue and red lines indicate the spin-up and spin-down, respectively. The Fermi level is set to be 0 eV.

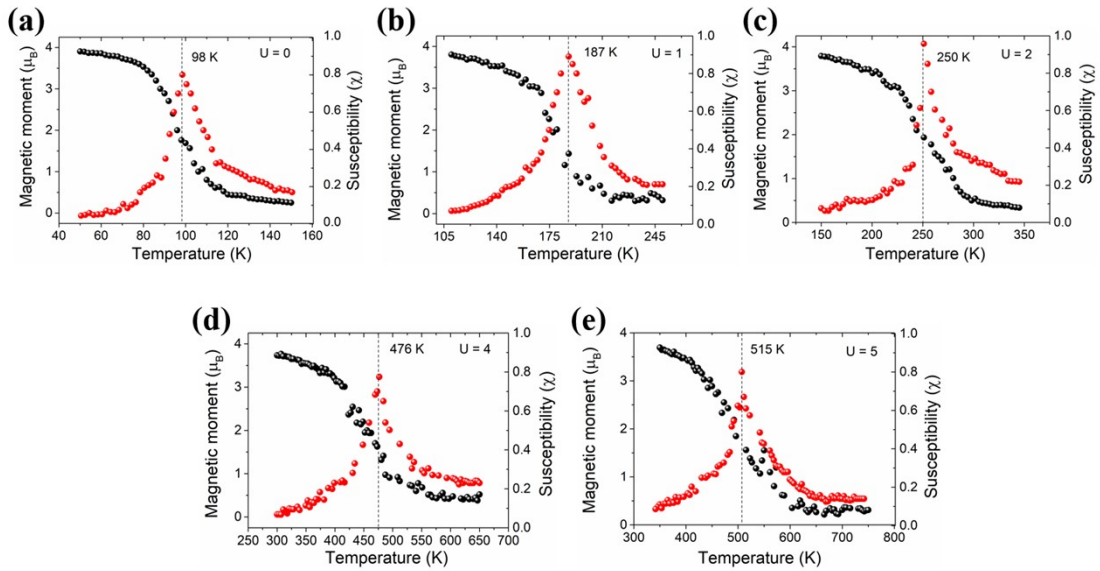


Fig. S4 Dependence of magnetic moment and magnetic susceptibility on the temperature by the Heisenberg model *via* Monte Carlo (MC) simulation of CrSc_2Te_4 monolayer with different U values.

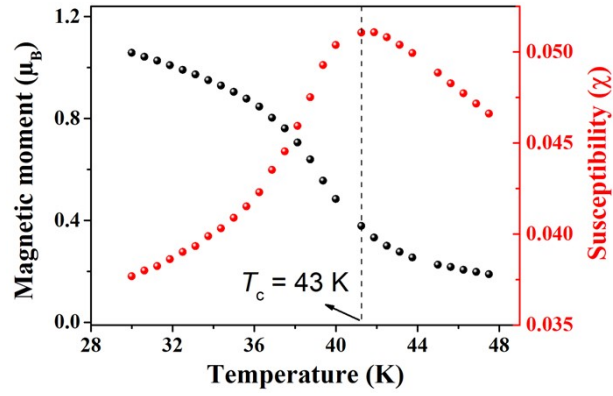


Fig. S5 Dependence of magnetic moment and magnetic susceptibility on the temperature by the Heisenberg model *via* Monte Carlo (MC) simulation of CrI₃ monolayer.

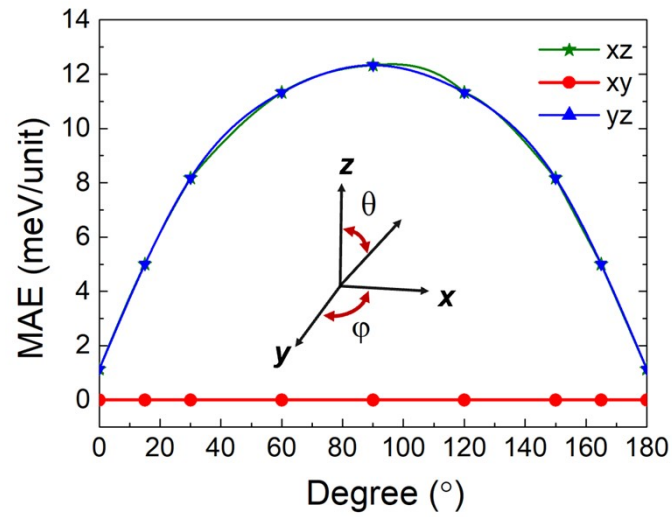


Fig. S6 The variation of magnetic anisotropy energy (MAE) of CrSc₂Te₄ monolayer. Among the MAE along the *xy* plane with respect to the polar angle φ , and along the *xz* and *yz* planes with respect to polar angle θ .

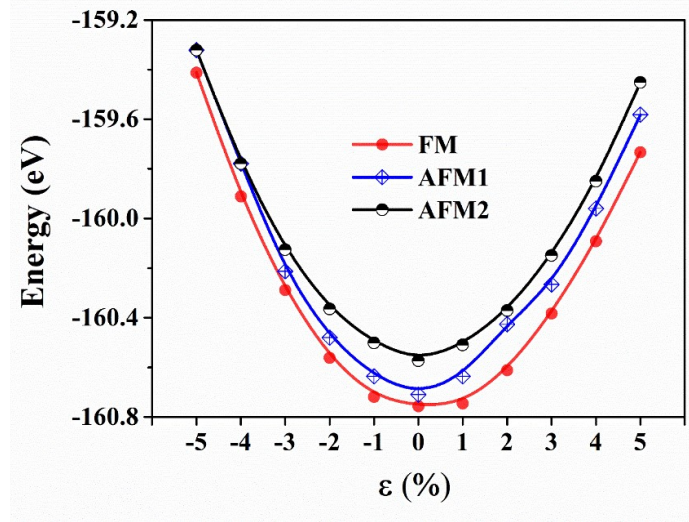


Fig. S7 The energies of different magnetic configurations as a function of strain range from -5% to 5% .

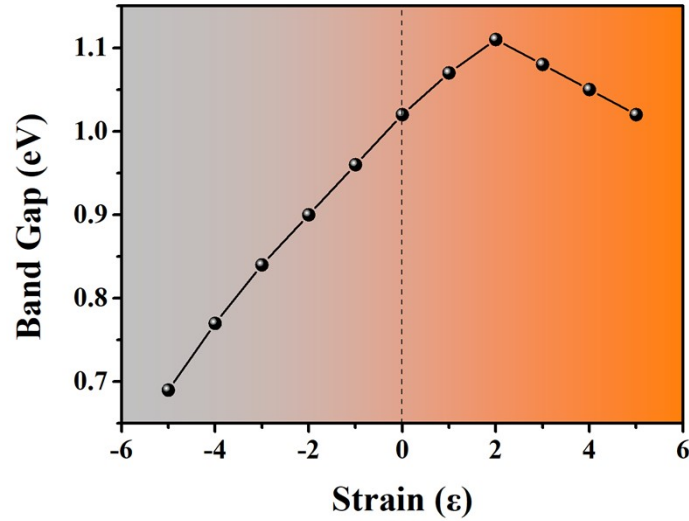


Fig. S8 The variation of band gap of CrSc_2Te_4 monolayer under strains (ε) from -5% to 5% using the PBE+ U method ($U = 3.0$ eV).

Table S1 The energy of three magnetic configurations with different U values using the PBE method.

| U | 0 | 1 | 2 | 3 | 4 | 5 |
|------|----------|----------|----------|----------|----------|----------|
| FM | -167.776 | -165.516 | -163.456 | -161.585 | -159.962 | -158.563 |
| AFM1 | -167.531 | -165.209 | -163.143 | -161.428 | -159.892 | -158.522 |
| AFM2 | -167.526 | -165.207 | -163.139 | -161.438 | -159.902 | -158.528 |

Table S2 Magnetic anisotropy energy (MAE, meV/Cr atom) per Cr atom between (100), (010) and (001) direction calculated for CrSc₂Te₄ monolayer by PBE+*U* (*U* from 0 to 5 eV) method.

| CrSc₂Te₄ | <i>E</i> (100)-<i>E</i> (001) | <i>E</i> (010)- <i>E</i> (001) | <i>E</i> (010)-<i>E</i> (100) |
|---------------------------------------|--------------------------------------|---------------------------------------|--------------------------------------|
| 0 | -0.428 | -0.428 | -0.002 |
| 1 | -0.792 | -0.794 | -0.001 |
| 2 | -1.342 | -1.351 | -0.003 |
| 3 | -2.451 | -2.458 | -0.007 |
| 4 | -1.206 | -1.201 | -0.001 |
| 5 | -1.490 | -1.493 | -0.003 |